




The effect of interleukin-17F on vasculogenic mimicry in oral tongue squamous cell carcinoma

Rabeia Almahmoudi^{1,2}  | Abdelhakim Salem^{1,2}  | Elin Hadler-Olsen^{3,4} |
Gunbjørg Svineng³ | Tuula Salo^{1,2,5,6,7} | Ahmed Al-Samadi^{1,2} 

¹Department of Oral and Maxillofacial Diseases, University of Helsinki, Helsinki, Finland

²Translational Immunology Research Program (TRIMM), University of Helsinki, Helsinki, Finland

³Department of Medical Biology, Faculty of Health Sciences, UiT The Arctic University of Norway, Tromsø, Norway

⁴The Public Dental Health Service Competence Center of Northern Norway, Tromsø, Norway

⁵Cancer and Translational Medicine Research Unit, University of Oulu, Oulu, Finland

⁶Medical Research Centre, Oulu University Hospital, Oulu, Finland

⁷Helsinki University Hospital, Helsinki, Finland

Correspondence

Rabeia Almahmoudi, Department of Oral and Maxillofacial Diseases, Faculty of Medicine, University of Helsinki; Biomedicum Helsinki 1, C223b P.O. Box 63 (Haartmaninkatu 8), 00014, Helsinki, Finland.
Email: rabeia.mustafa@helsinki.fi

Funding information

the Doctoral Program in Clinical Research (KLTO), Faculty of Medicine, University of Helsinki; the Emil Aaltonen Foundation; the Minerva Foundation of Medical Research; the Cancer Society of Finland; the Sigrid Jusélius Foundation; the Jane and Aatos Erkko Foundation

Abstract

Oral tongue squamous cell carcinoma (OTSCC) is one of the most common cancers worldwide and is characterized by early metastasis and poor prognosis. Recently, we reported that extracellular interleukin-17F (IL-17F) correlates with better disease-specific survival in OTSCC patients and has promising anticancer effects in vitro. Vasculogenic mimicry (VM) is the formation of an alternative vasculogenic system by aggressive tumor cells, which is implicated in treatment failure and poor survival of cancer patients. We sought to confirm the formation of VM in OTSCC and to investigate the effect of IL-17F on VM formation. Here, we showed that highly invasive OTSCC cells (HSC-3 and SAS) form tube-like VM on Matrigel similar to those formed by human umbilical vein endothelial cells. Interestingly, the less invasive cells (SCC-25) did not form any VM structures. Droplet-digital PCR, FACS, and immunofluorescence staining revealed the presence of CD31 mRNA and protein in OTSCC cells. Additionally, in a mouse orthotopic model, HSC-3 cells expressed VE-cadherin (CD144) but lacked Von Willebrand Factor. We identified different patterns of VM structures in patient samples and in an orthotopic OTSCC mouse model. Similar to the effect produced by the antiangiogenic drug sorafenib, IL-17F inhibited the formation of VM structures in vitro by HSC-3 and reduced almost all VM-related parameters. In conclusion, our findings indicate the presence of VM in OTSCC and the antitumorigenic effect of IL-17F through its effect on the VM. Therefore, targeting IL-17F or its regulatory pathways may lead to promising therapeutic strategies in patients with OTSCC.

KEYWORDS

Angiogenesis, CD31, Interleukin-17F, Oral tongue squamous cell carcinoma, Vasculogenic mimicry

Abbreviations: CD31, cluster of differentiation 31; DDP-PCR, droplet-digital PCR; FACS, fluorescence-activated cell sorting; HNSCC, head and neck squamous cell carcinoma; IL-17F, interleukin 17F; LYVE-1, lymphatic vessel endothelial hyaluronan receptor-1; OTSCC, oral tongue squamous cell carcinoma; PAS, periodic acid-Schiff; VEGF, vascular endothelial growth factor; VM, vasculogenic mimicry; VWF, Von Willebrand Factor.

This is an open access article under the terms of the Creative Commons Attribution-NonCommercial License, which permits use, distribution and reproduction in any medium, provided the original work is properly cited and is not used for commercial purposes.

© 2021 The Authors. *Cancer Science* published by John Wiley & Sons Australia, Ltd on behalf of Japanese Cancer Association.

1 | INTRODUCTION

Oral tongue squamous cell carcinoma (OTSCC) is the most common cancer in the oral cavity and its incidence is increasing worldwide.^{1,2} Unfortunately, the survival of patients with OTSCC has improved minimally in recent decades.^{3,4} The relatively high rates of tumor recurrence and metastasis to regional lymph nodes are considered the leading causes of disease-specific mortality.^{4,5} Therefore, identifying novel molecular targets that affect metastasis-related processes, such as vessel formation, is necessary to improve treatment outcomes of OTSCC patients.

Interleukin-17F (IL-17F), a member of IL-17 family, plays an important role in inflammatory and autoimmune diseases.⁶ Importantly, IL-17F was also shown to mediate antitumorigenic effects in cancers, including colon cancer and hepatocellular carcinoma.⁷⁻¹⁰ We have previously shown that extracellular IL-17F derived from mast cells, at the tumor invasive front, is associated with improved disease-specific survival in OTSCC patients.¹¹ Furthermore, we showed in a recent report that IL-17F exerted its antitumorigenic effects in OTSCC by inhibiting cancer cell proliferation and migration and endothelial cell tube formation.¹²

Vasculogenic mimicry (VM) is a model of tumor angiogenesis where tumor cells form intratumoral vessel-like channels to mediate tumor growth and metastasis.¹³ Recently, our meta-analysis revealed that VM is significantly associated with poor survival outcomes in head and neck squamous cell carcinoma (HNSCC) and esophageal cancer.¹⁴ The currently available angiogenesis inhibitors show limited clinical success in cancer treatment.¹⁵ This may partially be due to VM, which reduces the efficacy of antiangiogenic therapies.¹⁵ Therefore, VM was suggested as a potential promising therapeutic target in cancers, including OTSCC.^{13,14} Here, we sought to study the VM phenomenon in OTSCC and to further investigate the potential effect of IL-17F on the formation of VM structures by OTSCC cells.

2 | MATERIALS AND METHODS

2.1 | Cells and cell culture

We used the following OTSCC cell lines: HSC-3 (Japan Health Sciences Foundation), SCC-25 (American Type Culture Collection), and SAS (Japanese Collection of Research Bioresources) cells. We used human umbilical vein endothelial cells (HUVEC, Thermo Fisher Scientific) as a control for the tube formation assay. The culturing conditions were as previously reported.¹² Briefly, the high-invasive HSC-3 and SAS cell lines and the low-invasive SCC-25 cell lines were cultured in Dulbecco's modified Eagle's medium (DMEM)-12 (Gibco). Culture medium was supplied with 10% heat-inactivated fetal bovine serum (FBS), 100 U/ml penicillin, 100 µg/ml streptomycin, 250 ng/ml fungizone, 50 µg/ml ascorbic acid, and 0.1% hydrocortisone (all from Sigma-Aldrich). HUVEC were cultured in 75-cm² tissue-culture flasks using 200PRF medium (Thermo Fisher Scientific) supplemented with low-serum growth supplement (Thermo Fisher

Scientific), 100 U/ml penicillin (Sigma-Aldrich), and 100 µg/ml streptomycin (Sigma-Aldrich).

2.2 | Patient samples

In this study, we used paraffin-embedded samples from the pathology department of Oulu University Hospital. The samples were obtained from OTSCC patients ($n = 30$) who were treated surgically at the Oulu University Hospital during the period 1990-2010. The patients provided written informed consent before participating in the study. The data inquiry was approved by the National Supervisory Authority for Welfare and Health (VALVIRA) and the Ethics Committee of the Northern Ostrobothnia Hospital District.

2.3 | Orthotopic mouse model of OTSCC

The model was prepared as described previously.¹⁶ Briefly, subconfluent HSC-3 cells were detached and mixed with cold Matrigel 1:1 to a final concentration of 8×10^6 cells per ml. A cell suspension of 25 µl (2×10^5 cells) was injected into the lateral part of the tongue of 7-week-old BALB/c nude male mice (Charles River, Germany). On day 13, mice were sacrificed and tongues and draining lymph nodes were fixed in 4% paraformaldehyde (PFA) immediately after removal and were subsequently dehydrated and embedded in paraffin for further immunostaining. All experiments complied with the ARRIVE guidelines and were conducted in accordance with the European Convention for the Protection of Vertebrate Animals for Experimental and Other Scientific Purposes guidelines on accommodation and care of animals. The experiments were also approved by the Animal Welfare Committee at UiT-The Arctic University of Norway.

2.4 | Immunofluorescence staining

Oral tongue squamous cell carcinoma samples were cut to 5-µm thick sections. After deparaffinization in a xylene-ethanol series, slides were treated with heat-induced antigen retrieval using a microwave oven (MicroMED T/T Mega Histoprocessing Labstation; Milestone Srl). Next, slides were washed three times (5 minutes each) in phosphate-buffered saline (PBS) and then incubated in: (i) 10% donkey normal serum for 1 hour at room temperature (RT); (ii) 1:200 diluted monoclonal mouse anti-human pan-cytokeratin (M351501-2; Agilent Technologies) with 1:50 diluted polyclonal rabbit anti-human CD31 antibody (ab28364; Abcam), or 1:200 diluted polyclonal rabbit anti-human VE-Cadherin (CD144, ab232880; Abcam), or 1:1000 diluted polyclonal rabbit anti-human Von Willebrand Factor (VWF, ab6994; Abcam) overnight at 4°C; (iii) donkey anti-rabbit AlexaFluor-488 and donkey anti-mouse AlexaFluor-568 conjugated secondary antibodies for 1 hour at RT; and (iv) diamidino-2-phenylindole for 5 minutes at RT. Slides were washed three times for 5 minutes in dH₂O and samples were then mounted in Vector-Fluorescent Mounting Medium (Vector

Laboratories). For immunofluorescence staining of cells, OTSCC cells and HUVEC were cultured on Matrigel-coated coverslips. Next, the coverslips were washed with PBS and fixed using 4% PFA for 20 minutes at RT. Staining was performed using the same protocol described above. HUVEC were used as a positive control for CD31 staining. The primary antibodies were replaced with an antibody isotype control for negative control staining.

2.5 | Immunohistochemical and periodic acid-Schiff (PAS) staining

Slides were deparaffinized in a xylene-ethanol series and treated with Tris-EDTA pH 9 in a microwave oven (MicroMED T/T Mega Histoprocessing Labstation; Milestone Srl) for 15 minutes, followed by two 7-minute washes in PBS/Tween (PBST). Slides were blocked using Dako peroxidase blocking S2023 for 15 minutes at RT, followed by two PBST washes for 7 minutes each. Slides were incubated with 1:100 diluted polyclonal rabbit anti-human CD31 antibody (Abcam) for 1 hour at RT, followed by horseradish peroxidase (HRP) treatment for 30 minutes at RT. After two washes in PBST, slides were then treated with 3,3'-diaminobenzidine (Pierce™ DAB Substrate Kit, Thermo Fisher Scientific) for 5 minutes and washed with distilled water (dH₂O). Slides were incubated with 0.5% freshly prepared periodic acid for 10 minutes at RT and washed twice with dH₂O. Schiff stain was added for 15 minutes, followed by washing with running tap water for 15 minutes. Slides were stained with Cole's hematoxylin for 6 minutes, washed with running tap water for 10 minutes, rinsed with dH₂O, and mounted in Mountex (HistoLab).

2.6 | Droplet-digital PCR

Droplet-digital PCR (ddPCR) is a highly reliable technology that allows absolute quantification of specific targets and was performed as described previously.¹⁷ Briefly, the PCR reaction mix (20 µl) contained QX200™ EvaGreen® ddPCR™ Supermix (Bio-Rad Laboratories), complementary DNA (cDNA) and CD31 primers. CD31 primers were forward: 5'-AACAGTGTGACATGAAGAGCC-3' and reverse: 5'-TGTA AACAGCAGCAGTCATCCTT-3'. Samples were loaded into a droplet generator cartridge with 70 µl of EvaGreen droplet generation oil. Next, sample droplets were pipetted into a ddPCR™ 96-well plate, sealed in PX1-PCR plate sealer, and loaded into a T100 thermal cycler with annealing temperature set to 60°C. The plate was then transferred into the droplet reader using QX200™ Droplet Digital™ PCR Systems (Bio-Rad Laboratories). The data were analyzed using QuantaSoft software version 1.7.4.0917 (Bio-Rad Laboratories).

2.7 | Flow cytometry

The endothelial cell marker CD31 was identified using fluorescence-activated cell sorting (FACS) analysis. Cultured HUVEC, HSC-3, SAS,

and SCC-25 cell lines were fixed with 4% PFA as above, then permeabilized with 0.1% Triton-X for 10 minutes at RT, followed by three washes with PBS. Next, cells were incubated with 4 µl Alexa Fluor® 488 monoclonal mouse anti-human CD31 (ab187594; Abcam) for 30 minutes in dark at RT. After three washes with PBS, cells were centrifuged at 400 g for 5 minutes, resuspended in 1 ml of ice-cold PBS, and run on a BD influx sorter (BD).

2.8 | Tube formation assay

The tube formation assay was performed as previously described.¹² Briefly, a total amount of 100 µl of Matrigel® (Corning) was added to 24-well plates and incubated for 30 minutes at 37°C. Cells were seeded at a density of 8×10^4 cells/well for HUVEC and 12×10^4 cells/well for OTSCC cells. The cells were cultured in media supplied with and without IL-17F at a concentration of 10, 50, or 100 ng/ml based on our previous study.¹² In addition, HSC-3 cells were also treated with sorafenib (LC Laboratories) at a concentration of 1, 2.5, or 5 µM. Cells were incubated for 8 hours (HUVEC) or 24 hours (OTSCC cells) at 37°C, and images of tube formation were taken accordingly.

2.9 | Microscopy and image analysis

Imaging for immunofluorescence and immunohistochemical staining was performed using a Leica DM6000 microscope and a Leica TCS SP8 confocal microscope (Leica Microsystems) using magnification powers 20x, 40x, and 63x. Cell culture imaging was performed using a Nikon Eclipse TS100 inverted microscope (Nikon Instruments). Images from tube formation assay were analyzed using ImageJ software (Wayne Rasband, National Institute of Health).

2.10 | Statistical analysis

Experiments were performed independently at least three times. Values are expressed as means ± standard deviation. Data were analyzed using IBM SPSS Statistics version 24.0 (IBM Corp.). Statistical significance was determined using the Mann-Whitney *U* test and Friedman test on independent samples. Statistical significance was set at $P < .05$.

3 | RESULTS

3.1 | OTSCC cells form tube-like structures on Matrigel

We first tested whether all OTSCC cells can form tube-like networks on a three-dimensional matrix (ie, Matrigel) similar to HUVEC. Interestingly, HSC-3 and SAS cell lines formed distinct

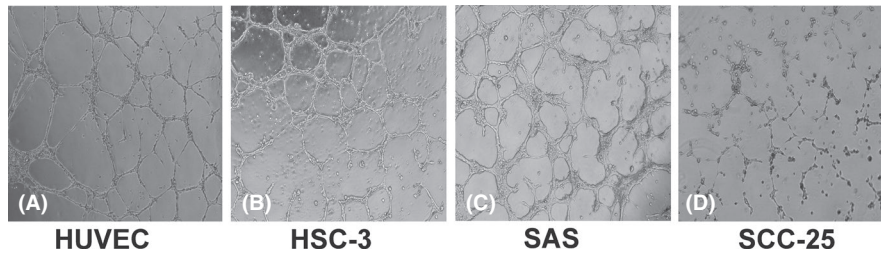


FIGURE 1 Cancer cells form tube-like structures on Matrigel. A-C, The high-invasive oral tongue squamous cell carcinoma (OTSCC) cell lines (HSC-3 and SAS) formed interconnected tube-like structures that were similar to the structures formed by human umbilical vein endothelial cells (HUVEC) on Matrigel. D, The low-invasive OTSCC cells (SCC-25) did not form any consistent tube-like structures when cultured under the same conditions. Magnification: 4X

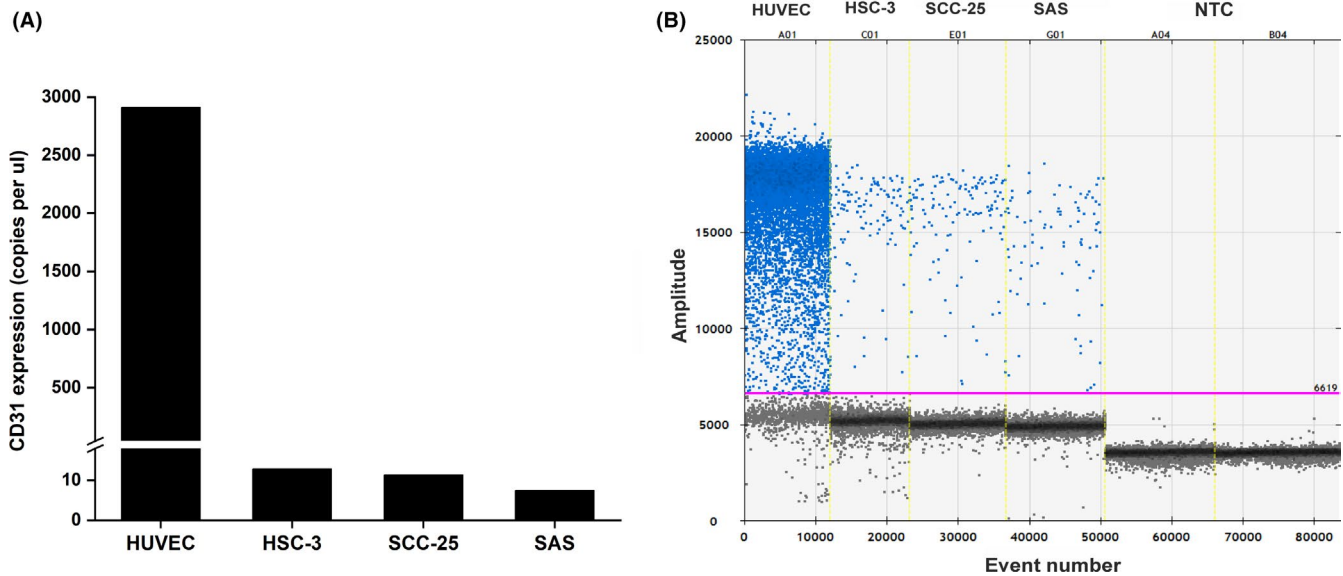


FIGURE 2 Gene analysis of CD31 in tumor cells. Absolute quantification by droplet-digital PCR revealed positive expression of CD31 in oral tongue squamous cell carcinoma (OTSCC) cells HSC-3, SCC-25, and SAS in vitro (average of approximately 10 copies/ μ l), which was expectedly less than the control (human umbilical vein endothelial cells; HUVEC)

interconnected tube-like structures that were similar to the tubes formed by HUVEC (Figure 1A-C). However, low-invasive OTSCC cells (SCC-25) did not form any consistent tube-like structures when cultured under the same conditions; the cells remained in small cell aggregates (Figure 1D).

3.2 | OTSCC cell lines express CD31 in vitro

We performed DDPCR to determine if OTSCC cells express the endothelial cell marker CD31 in vitro. Interestingly, all these cell lines showed a positive expression of CD31 (average 10 copies/ μ l), although it was much less than the positive control (HUVEC) (Figure 2A, B). Immunofluorescence staining showed that, similar to HUVEC, these cells stained positive for CD31 (Figure 3A). We performed FACS analysis to further confirm these findings. The number of CD31⁺ cells in HSC-3 (90%) was almost the same as in HUVEC

(96%), whereas only 44% of SCC-25 and 1.8% of SAS cells were positive (Figure 3B; and Figure S1).

3.3 | Different VM patterns identified in patient samples

We used the following two staining approaches to study the formation of VM in OTSCC patient samples: PAS-CD31 assay and double-label pan-cytokeratin-CD31 immunofluorescence. Interestingly, we identified two different VM-related patterns in OTSCC patient samples, namely PAS⁺/CD31⁻ and pan-cytokeratin⁺/CD31⁺ vessel-like structures. In addition to the PAS⁺/CD31⁻ VM vessels (Figure 4A; blue arrow), PAS⁺/CD31⁺ blood vessels were also found in the tumor microenvironment (TME; Figure 4A; black arrow heads). The pan-cytokeratin⁺/CD31⁺ structures (ie, mosaic pattern) were detected as intratumoral vessel-like channels (Figure 4B).

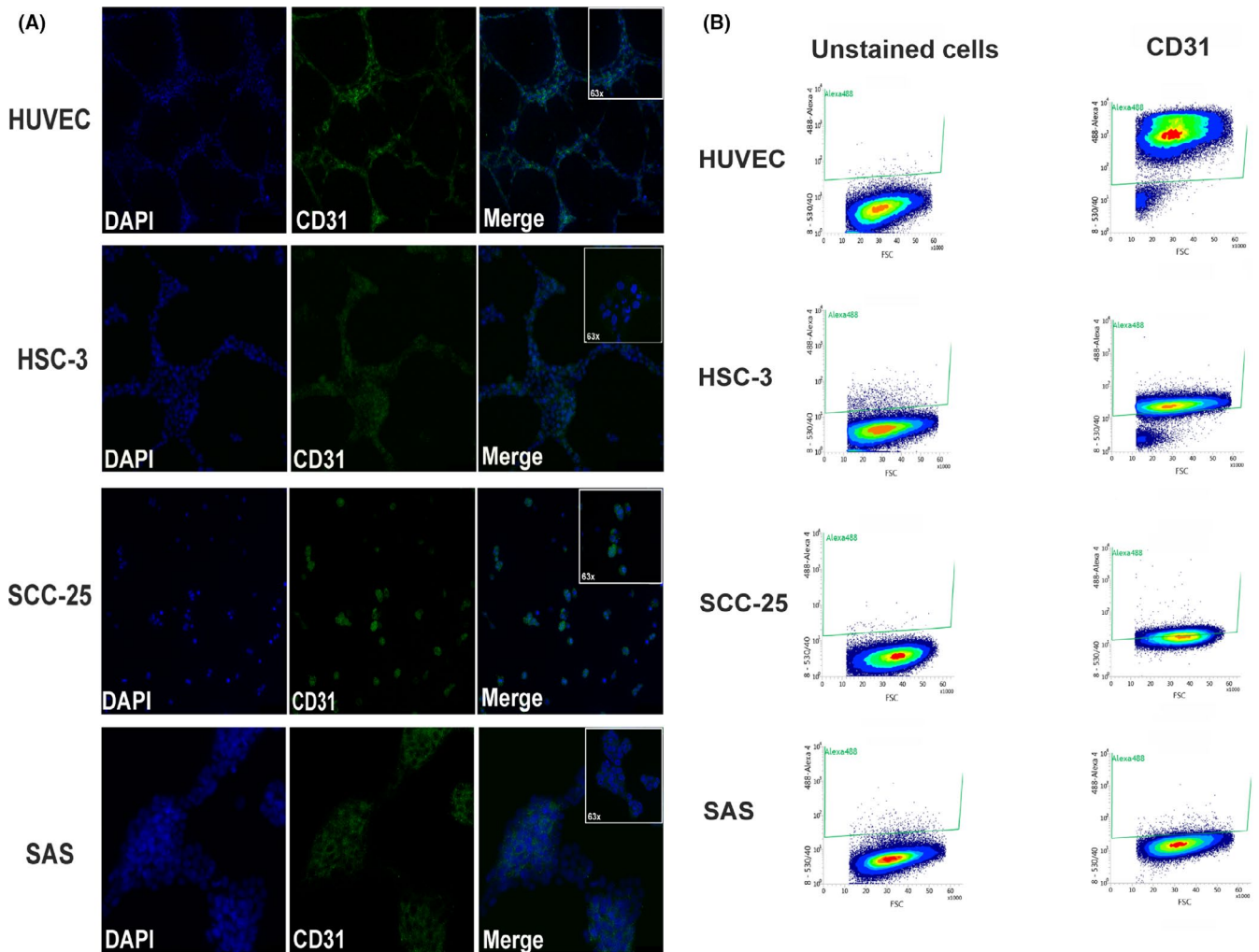


FIGURE 3 Double-label immunofluorescence and FACS analysis of CD31. A, Cultured oral tongue squamous cell carcinoma (OTSCC) cell lines showed distinct positive staining of CD31. Magnification: 20 \times and 63 \times . B, Representative profiles from FACS of OTSCC cells revealed a CD31 expression level of 96% (human umbilical vein endothelial cells; HUVEC), 90% (HSC-3), 44% (SCC-25), and 1.8% (SAS)

3.4 | OTSCC formed VM structures in orthotopic mouse model

To confirm our findings in an *in vivo* model, we injected HSC-3 cells into the lateral border of the tongue of 7-week-old BALB/c nude male mice as described above. Samples were stained using double immunofluorescence staining against human pan-cytokeratin and several endothelial cell markers, including CD31, VE-cadherin (CD144), and VWF. Interestingly, we detected human CD31-positive vessels within and adjacent to the tumor area, which also contained red blood cells (Figure 5A, B; arrows). These human CD31⁺ vessels were absent in the adjacent mouse tissue, thus confirming the specificity of the staining antibody (Figure 5C, arrows). The presence of CD31⁺ vessels was further confirmed by confocal microscopy (Figure 5D, arrow). Interestingly, HSC-3 cells were CD144⁺ regardless of the presence or absence of VM. On the other hand, HSC-3 cells were all negative for VWF (Figure 5E-F, respectively). Our staining also showed that the vessels formed by the HSC-3 were most likely functional, as we could identify some red blood cells within the tubes (Figure. S2).

3.5 | IL-17F reduces VM formation *in vitro*

Recently, we showed that OTSCC cells express IL-17F receptors (IL-17RA and IL-17RC) and that IL-17F has antitumorigenic effects by reducing tube formation of HUVEC.¹² To determine if IL-17F has a similar effect on VM, we cultured HSC-3 cells on Matrigel and incubated them with or without different concentrations of IL-17F. The inhibitory effect of IL-17F on VM was compared with sorafenib, which is an angiogenesis inhibitor currently used for the treatment of various human cancers. As expected, we observed a significant reduction in tube formation by HSC-3 cells following treatment with sorafenib for 24 hours (Figure 6A). The inhibitory effect of sorafenib was observed at concentrations of 1–5 μ M. Interestingly, treatment with IL-17F produced similar inhibitory effects on the formation of tube-like structures in HSC-3 cells compared with control. The clearest inhibitory effect of IL-17F on VM was observed at a concentration of 100 ng/ml, which mimicked the sorafenib-mediated effect at 1 μ M (Figure 6A).

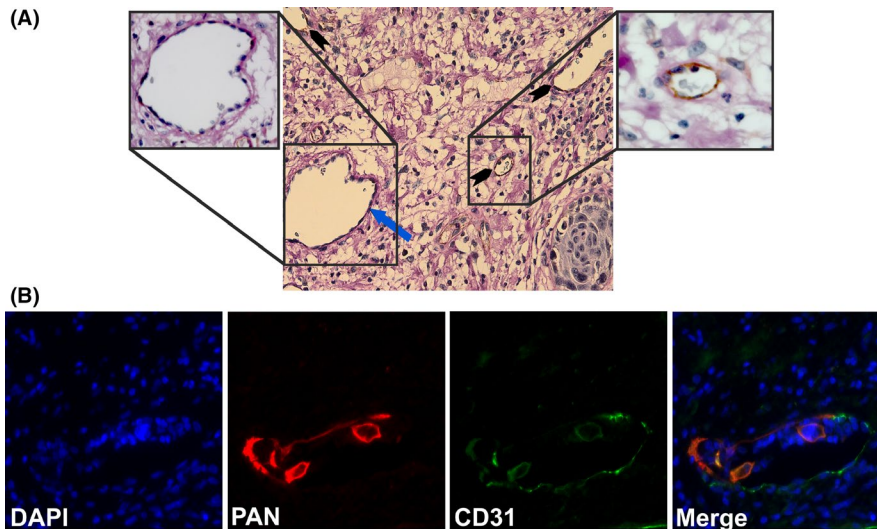


FIGURE 4 Identification of vasculogenic mimicry (VM) structures in oral cancer patients. A, Identification of PAS⁺/CD31⁻ VM structures. Paraffin-embedded resection samples from oral tongue squamous cell carcinoma (OTSCC) patients were stained with anti-human CD31 (brown), periodic acid-Schiff (PAS: pink), and hematoxylin (purple). PAS⁺/CD31⁻ vessel-like structures (blue arrow) and PAS⁺/CD31⁺ blood vessels (black arrow heads) were identified. Magnification: 40 \times . B, Identification of pan-cytokeratin⁺/CD31⁺ mosaic pattern of VM. Pan-cytokeratin⁺/CD31⁺ mosaic structures of VM in OTSCC patients (pan-cytokeratin: red; CD31: green)

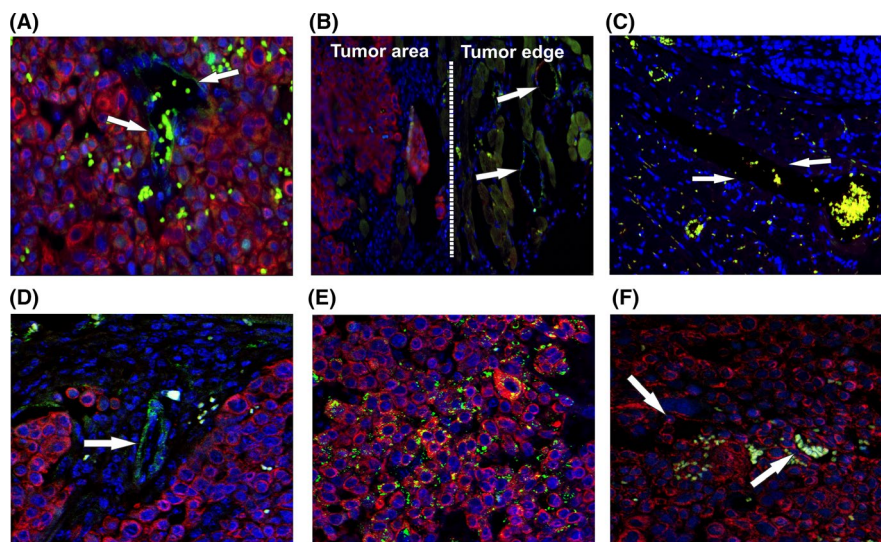
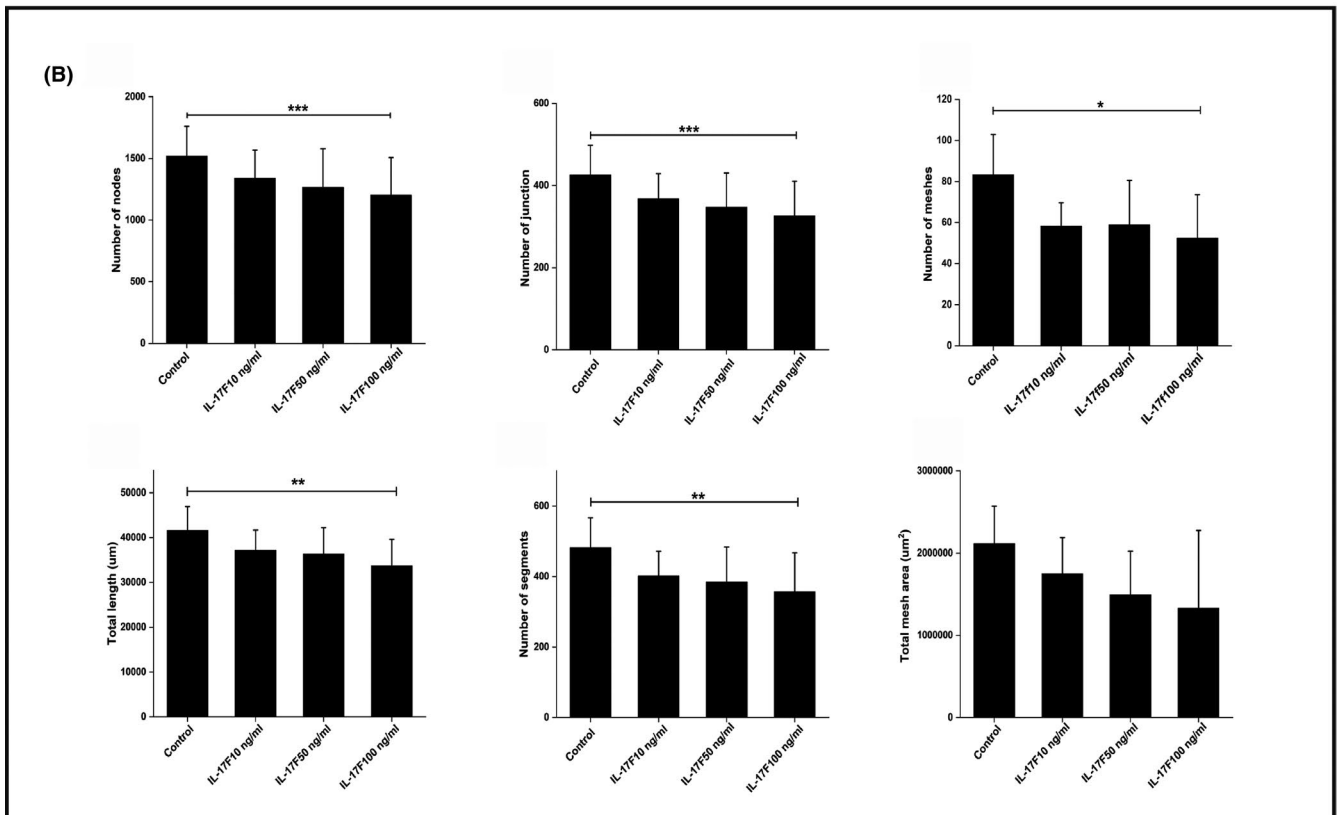
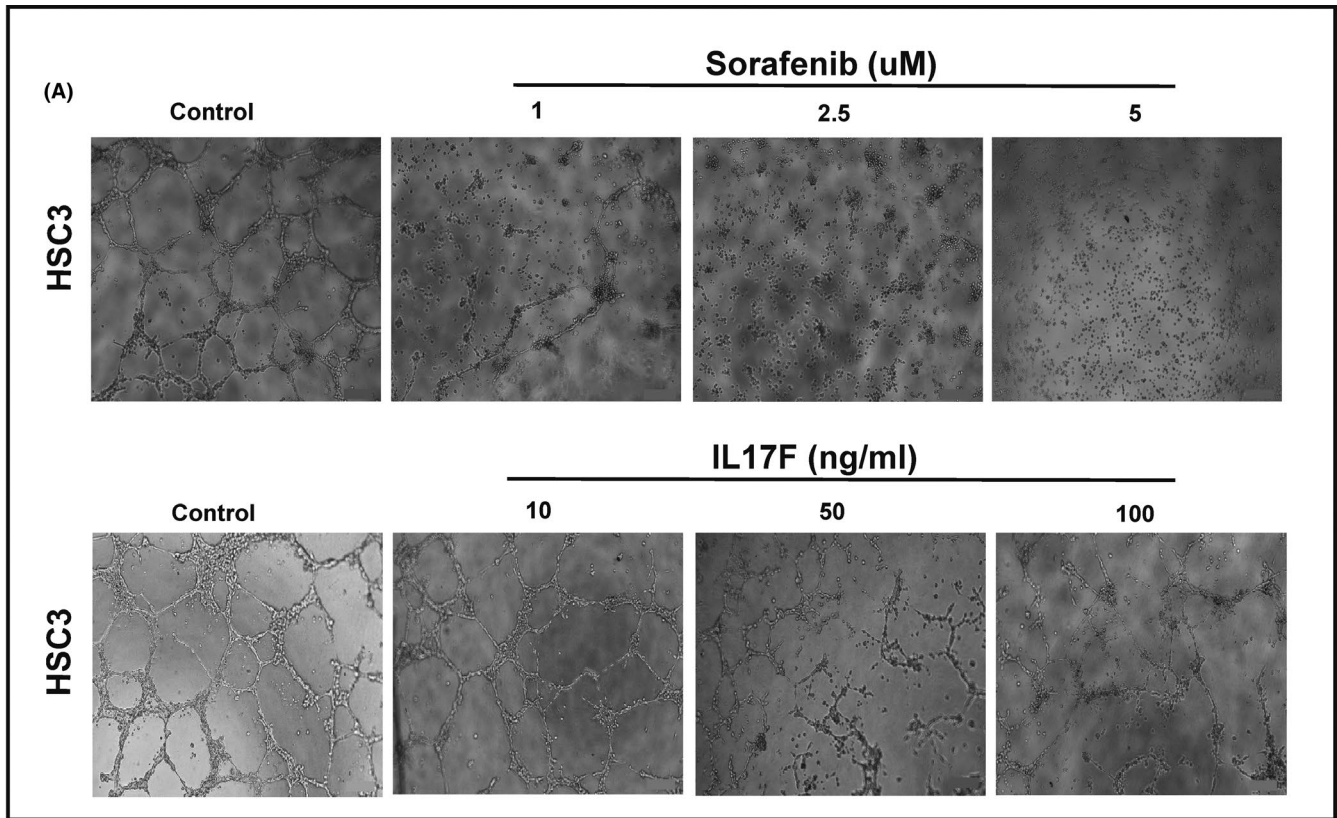


FIGURE 5 Identification of VM structures in an orthotopic mouse model of oral cancer. A, Surgical specimens of an orthotopic mouse model of oral tongue squamous cell carcinoma (OTSCC) showed formation of vessels positive for human CD31 (pan-cytokeratin: red; CD31: green) within and adjacent to the tumor area (arrows). B-C, Human CD31⁺ vessels were not found in the adjacent mouse tissue (arrows). D, Confocal microscopy confirmed the presence of CD31⁺ vessels in vivo. E, Human tumor cells showed abundant staining intensity of CD144 (VE-cadherin). F, No evident staining pattern of Von Willebrand factor was observed in the orthotopic mouse model of OTSCC (green: red blood cell autofluorescence). Magnification: 40 \times

FIGURE 6 A, Interleukin-17F inhibits formation of vasculogenic mimicry (VM) in vitro. The effect of IL-17F on VM formation on Matrigel was compared with the angiogenesis inhibitor sorafenib. When treated with sorafenib for 24 h, HSC-3 cells showed reduction in tube formation at concentrations of 1-5 μ M. Similarly, IL-17F inhibited the formation of the tube-like structures in HSC-3 cells compared with control, with the greatest effect observed at 100 ng/ml. Magnification: 4 \times . B, Interleukin-17F reduces the parameters of VM in vitro. A tube formation analysis tool was used to further analyze the IL-17F effect on VM parameters. IL-17F at 100 ng/ml reduced almost all VM-related parameters in HSC-3, including number of nodes ($P = .001$), number of junctions ($P = .001$), number of meshes ($P = .02$), total length ($P = .004$), and number of segments ($P = .009$). Total mesh areas were also reduced by IL-17F, but the difference was not significant compared with the controls. Experiments were performed independently at least three times. Values are expressed as means \pm SD. Mann-Whitney U test and Friedman test were performed on independent samples



Next, we used the tube formation analysis assay to further determine the effect of IL-17F on VM parameters. IL-17F at 100 ng/ml reduced almost all VM-related parameters in HSC-3, including

number of nodes ($P = .001$), number of junctions ($P = .001$), number of meshes ($P = .02$), total length ($P = .004$), and number of segments ($P = .009$). Although total mesh areas were also reduced by

IL-17F, the difference was not significant compared with controls (Figure 6B).

4 | DISCUSSION

Oral tongue squamous cell carcinoma is one of the most common forms of HNSCC and is characterized by rapid growth and metastasis.^{1,2} To grow and metastasize, tumor cells interact with various cellular and molecular constituents of the TME, including inflammatory cells, endothelial cells, and cytokines, among others.¹⁷ One of the most important aspects of TME interaction is to provide tumor cells with sufficient nutritional support by inducing angiogenesis, which promotes invasion and metastasis.^{18,19} In addition to tumor-induced angiogenesis ("neoangiogenesis"), VM was identified as a tumor microcirculation model, where tumor cells can form de novo vessel-like channels independently from endothelial cells.^{20,21} Importantly, we showed in a recent meta-analysis that HNSCC patients with positive VM had significantly shorter overall survival than VM-negative patients.¹⁴

The TME profile influences patient prognosis and significantly impacts the efficacy of anticancer therapies, therefore providing a wide range of promising therapeutic targets.¹⁸ In this regard, we showed that positive expression of mast cell-derived extracellular IL-17F at the invasive front correlated with better overall survival of OTSCC patients.¹¹ Furthermore, we recently reported that OTSCC cells express IL-17F receptors (IL-17RA and IL-17RC) and that IL-17F reduced OTSCC cell proliferation and strongly suppressed HUVEC tube formation.¹² In many aggressive cancers, including OTSCC, tumor cells are able to tolerate harsh microenvironmental conditions such as the immune cell responses and hypoxia. The VM represents one of these important "evasion" pathways.¹³ Therefore, it is important to identify new molecules for targeting VM for therapeutic purposes. Here, we further demonstrated that IL-17F has an inhibitory effect on HSC3 cell-formed VM structures in vitro.

The formation of VM in a 3D culture has been shown in different cancer cells, including those from primary and metastatic OTSCC.²² Here, we confirmed the ability of certain invasive OTSCC cells (HSC-3 and SAS cells) to form VM structures on Matrigel, where they formed capillary-like networks similar to HUVEC. Interestingly, the less invasive SCC-25 cells were unable to form tube-like structures, which supports the observation that VM is more commonly encountered in aggressive tumors.²³ A strong immunoreactivity of endothelium-related proteins (CD31 and CD34) has been identified in human aggressive cancer cells, such as melanoma and gastric adenocarcinoma, which suggests that these proteins play a role in VM formation.^{24,25} In particular, CD31 is an integral membrane protein that has also been found in robust stem cells, which induced strong vasculogenic properties in blood-derived CD31⁺ cells.^{26,27} Consistent with this, DDPCR and immunofluorescence staining showed that the cultured OTSCC cell lines were CD31⁺. However, although SAS cells expressed CD31 mRNA and formed distinct VM

in vitro, they were negative for CD31 when analyzed using FACS. Additionally, when injected in mice tongue, a large percentage of HSC-3 cells, even without tube formation, were CD144⁺ and some were CD31⁺. VE-cadherin is believed to be specific for endothelial cells and has also been found in a wide variety of aggressive tumors and is linked with VM formation.²⁸ VWF was not expressed by HSC-3 cells. These findings could partly be related to differences in nutrient and oxygen supply between the in vivo environment and in vitro assays.²⁹

VM was initially identified as PAS-positive/CD31⁻ or CD34⁻ vessel-like channels lined by tumor cells.³⁰ However, this concept has been further promoted with recognition of the mosaic vessel model, where the luminal surface is lined by both cancer cells and endothelial cells.³¹ This is supported by the plasticity of cancer stem cells to transdifferentiate into vascular endothelial-like cells and to induce VM in aggressive cancers, such as glioblastoma.³² Furthermore, we observed that the invasive OTSCC cell line, HSC-3, expresses a functional lymphatic endothelial cell marker (ie, LYVE-1), which can influence cell migration and vessel-like network formation.³³ In the present study, we identified both the mosaic model (pancytokeratin⁺/CD31⁻) and classical PAS⁺/CD31⁻ vessel-like structures in OTSCC patient samples. Importantly, we also detected the formation of a vessel-like pattern in the orthotopic animal model, which supports previous reports on the ability of cancer stem cells to form VM in vivo.^{34,35} Thus, our findings suggest that in addition to the traditional PAS⁺/CD31⁻ pattern, the mosaic model is also important when identifying VM structures.

Recently, we reported that IL-17F has promising anticancer properties in vitro by inhibiting tube formation of cultured HUVEC in a dose-dependent manner.¹² Here, we sought to further investigate such effect of IL-17F in vitro compared with an FDA-approved angiogenesis inhibitor. We used the kinase inhibitor sorafenib because of its ability to inhibit the VEGF receptor family, which is involved in tumor angiogenesis and progression.³⁶⁻³⁸ In this context, it is interesting that IL-17F produced a significant reduction in HSC-3-formed VM structures similar to sorafenib. The peak inhibitory effect of IL-17F was observed at 100 ng/ml, which is the same concentration that produced the most promising anticancer effects in our previous in vitro assays. We have shown that IL-17F at this concentration reduced the proliferation and random migration of HSC-3 cells.¹² However, this effect on tongue cancer cell proliferation was modest (16%), which most likely is not sufficient to explain the effects on tube formation. In this regard, IL-17F has been shown to downregulate key proangiogenic cytokines, such as IL-6, IL-8, and VEGF, which could inhibit tumor angiogenesis.⁹ Another study indicated that IL-17F plays a potent inhibitory role in tumorigenesis in vivo by influencing VEGF levels and CD31⁺ cells, leading to inhibition of tumor angiogenesis.⁷

In conclusion, we confirmed previous reports about VM in in vitro and in vivo and provided evidence on the presence of two VM patterns in OTSCC. We also demonstrated that IL-17F exhibits a potential therapeutic effect in OTSCC by inhibiting cancer cell-formed VM structures in vitro. In fact, the inhibition of VM could halt tumor

progression and could therefore provide an important therapeutic approach.²⁰ This appears consistent with the promising anticancer effects of IL-17F. However, we acknowledge several limitations in our report, such as the lack of perfusion analysis to verify VM functionality. Furthermore, the inhibitory effect of IL-17F on the formation of VM needs to be assessed in an appropriate in vivo model. Therefore, further studies are warranted to investigate the mechanistic effects of IL-17F on VM in OTSCC.

ACKNOWLEDGEMENTS

The authors acknowledge the funders of this study: the Doctoral Program in Clinical Research (KLTO), Faculty of Medicine, University of Helsinki; the Emil Aaltonen Foundation; the Minerva Foundation of Medical Research; the Cancer Society of Finland; the Sigrid Jusélius Foundation, and the Jane and Aatos Erkko Foundation. The authors would like to thank Antti Isomäki (Biomedicum Imaging Unit, University of Helsinki) and Noora Aarnio (Biomedicum Flow Cytometry Unit, University of Helsinki) for their kind assistance.

DISCLOSURE

The authors have no conflict of interest.

ORCID

Rabeia Almahmoudi  <https://orcid.org/0000-0002-5336-7258>

Abdelhakim Salem  <https://orcid.org/0000-0002-9455-3823>

Ahmed Al-Samadi  <https://orcid.org/0000-0003-1938-2136>

REFERENCES

- Miranda-Filho A, Bray F. Global patterns and trends in cancers of the lip, tongue and mouth. *Oral Oncol.* 2020;24(102):104551. <https://doi.org/10.1016/j.oraloncology.2019.104551>
- Kim YJ, Kim JH. Increasing incidence and improving survival of oral tongue squamous cell carcinoma. *Sci Rep.* 2020;10(1):7877. <https://doi.org/10.1038/s41598-020-64748-0>
- Ng JH, Iyer NG, Tan MH, Edgren G. Changing epidemiology of oral squamous cell carcinoma of the tongue: a global study. *Head Neck.* 2016;39:297-304.
- Van Dijk BA, Brands MT, Geurts SM, Merx MA, Roodenburg JL. Trends in oral cavity cancer incidence, mortality, survival and treatment in the Netherlands. *Int J Cancer.* 2016;139:574-583.
- da Silva SD, Hier M, Mlynarek A, Kowalski LP, Alaoui-Jamali MA. Recurrent oral cancer: current and emerging therapeutic approaches. *Front Pharmacol.* 2012;30:149.
- Kuwabara T, Ishikawa F, Kondo M, Kakiuchi T. The Role of IL-17 and related cytokines in inflammatory autoimmune diseases. *Mediators Inflamm.* 2017;2017:3908061. <https://doi.org/10.1155/2017/3908061>
- Tong Z, Yang XO, Yan H, et al. A protective role by interleukin-17F in colon tumorigenesis. *PLoS One.* 2012;7(4):e34959. <https://doi.org/10.1371/journal.pone.0034959>
- Al-Samadi A, Moossavi S, Salem A, et al. Distinctive expression pattern of interleukin-17 cytokine family members in colorectal cancer. *Tumor Biol.* 2015;37:1609-1615.
- Xie Y, Sheng W, Xiang J, Ye Z, Yang J. Interleukin-17F suppresses hepatocarcinoma cell growth via inhibition of tumor angiogenesis. *Cancer Invest.* 2010;28(6):598-607. <https://doi.org/10.3109/07357900903287030>
- Ding L, Hu EL, Xu YJ, et al. Serum IL-17F combined with VEGF as potential diagnostic biomarkers for oral squamous cell carcinoma. *Tumor Biol.* 2015;36:2523-2529.
- Almahmoudi R, Salem A, Sieviläinen M, et al. Extracellular interleukin-17F has a protective effect in oral tongue squamous cell carcinoma. *Head Neck.* 2018;40(10):2155-2165. <https://doi.org/10.1002/hed.25207>
- Almahmoudi R, Salem A, Murshid S, et al. Interleukin-17F has anti-tumor effects in oral tongue cancer. *Cancers (Basel).* 2019;11(5):650. <https://doi.org/10.3390/cancers11050650>
- Zhang X, Zhang J, Zhou H, Fan G, Li Q. Molecular mechanisms and anticancer therapeutic strategies in vasculogenic mimicry. *J Cancer.* 2019;10(25):6327-6340. <https://doi.org/10.7150/jca.34171>
- Hujanen R, Almahmoudi R, Karinen S, Nwaru BI, Salo T, Salem A. A promising prognosticator in head and neck squamous cell carcinoma and esophageal cancer? A systematic review and meta-analysis. *Cells.* 2020;9(2):507.
- Ribatti D, Annese T, Ruggieri S, Tamma R, Crivellato E. Limitations of anti-angiogenic treatment of tumors. *Transl Oncol.* 2019;12(7):981-986. <https://doi.org/10.1016/j.tranon.2019.04.022>
- Åström P, Juurikka K, Hadler-Olsen ES, et al. The interplay of matrix metalloproteinase-8, transforming growth factor- β 1 and vascular endothelial growth factor-C cooperatively contributes to the aggressiveness of oral tongue squamous cell carcinoma. *Br J Cancer.* 2017;117(7):1007-1016. <https://doi.org/10.1038/bjc.2017.249>
- Salem A, Almahmoudi R, Hagström J, et al. Human β -Defensin 2 expression in oral epithelium: potential therapeutic targets in oral lichen planus. *Int J Mol Sci.* 2019;20(7):1780. <https://doi.org/10.3390/ijms20071780>
- Roma-Rodrigues C, Mendes R, Baptista PV, Fernandes AR. Targeting tumor microenvironment for cancer therapy. *Int J Mol Sci.* 2019;20(4):840. <https://doi.org/10.3390/ijms20040840>
- Pickup MW, Mouw JK, Weaver VM. The extracellular matrix modulates the hallmarks of cancer. *EMBO Rep.* 2014;15(12):1243-1253. <https://doi.org/10.15252/embr.201439246>
- Luo Q, Wang J, Zhao W, et al. Vasculogenic mimicry in carcinogenesis and clinical applications. *J Hematol Oncol.* 2020;13(1):19. <https://doi.org/10.1186/s13045-020-00858-6>
- Maniotis AJ, Folberg R, Hess A, et al. Vascular channel formation by human melanoma cells in vivo and in vitro: vasculogenic mimicry. *Am J Pathol.* 1999;155(3):739-752. [https://doi.org/10.1016/S0002-9440\(10\)65173-5](https://doi.org/10.1016/S0002-9440(10)65173-5)
- Upile T, Terjes W, Radhi H, et al. Vascular mimicry in cultured head and neck tumour cell lines. *Head Neck Oncol.* 2011;23(3):55. <https://doi.org/10.1186/1758-3284-3-55>
- Ge H, Luo H. Overview of advances in vasculogenic mimicry - a potential target for tumor therapy. *Cancer Manag Res.* 2018;2(10):2429-2437. <https://doi.org/10.2147/CMAR.S164675>
- Kim HS, Won YJ, Shim JH, et al. Morphological characteristics of vasculogenic mimicry and its correlation with EphA2 expression in gastric adenocarcinoma. *Sci Rep.* 2019;9(1):3414. <https://doi.org/10.1038/s41598-019-40265-7>
- Pisacane AM, Picciotto F, Risio M. CD31 and CD34 expression as immunohistochemical markers of endothelial transdifferentiation in human cutaneous melanoma. *Cell Oncol.* 2007;29(1):59-66. <https://doi.org/10.1155/2007/486579>
- Kim SW, Kim H, Cho HJ, Lee JU, Levit R, Yoon YS. Human peripheral blood-derived CD31+ cells have robust angiogenic and vasculogenic properties and are effective for treating ischemic vascular disease. *J Am Coll Cardiol.* 2010;56(7):593-607. <https://doi.org/10.1016/j.jacc.2010.01.070>
- Li ZJ, Wang ZZ, Zheng YZ, et al. Kinetic expression of platelet endothelial cell adhesion molecule-1 (PECAM-1/CD31) during embryonic stem cell differentiation. *J Cell Biochem.* 2005;95(3):559-570. <https://doi.org/10.1002/jcb.20436>

28. Fernández-Cortés M, Delgado-Bellido D, Oliver FJ. Vasculogenic Mimicry: Become an Endothelial Cell "But Not So Much". *Front Oncol*. 2019;22(9):803. <https://doi.org/10.3389/fonc.2019.00803>
29. Ahmadiankia N. In vitro and in vivo studies of cancer cell behavior under nutrient deprivation. *Cell Biol Int*. 2020;44(8):1588-1597. <https://doi.org/10.1002/cbin.11368>
30. Folberg R, Hendrix MJ, Maniotis AJ. Vasculogenic mimicry and tumor angiogenesis. *Am J Pathol*. 2000;156(2):361-381. [https://doi.org/10.1016/S0002-9440\(10\)64739-6](https://doi.org/10.1016/S0002-9440(10)64739-6)
31. Chang YS, di Tomaso E, McDonald DM, Jones R, Jain RK, Munn LL. Mosaic blood vessels in tumors: frequency of cancer cells in contact with flowing blood. *Proc Natl Acad Sci U S A*. 2000;97(26):14608-14613. <https://doi.org/10.1073/pnas.97.26.14608>
32. Scully S, Francescone R, Faibish M, et al. Transdifferentiation of glioblastoma stem-like cells into mural cells drives vasculogenic mimicry in glioblastomas. *J Neurosci*. 2012;32(37):12950-12960. <https://doi.org/10.1523/JNEUROSCI.2017-12.2012>
33. Karinen S, Juurikka K, Hujanen R, et al. Tumour cells express functional lymphatic endothelium-specific hyaluronan receptor in vitro and in vivo: lymphatic mimicry promotes oral oncogenesis?. *Oncogenesis*. 2021;10(3):23. <https://doi.org/10.1038/s41389-021-00312-3>
34. Gao S, Fan C, Huang H, Zhu C, Su M, Zhang Y. Effects of HCG on human epithelial ovarian cancer vasculogenic mimicry formation in vivo. *Oncol Lett*. 2016;12(1):459-466. <https://doi.org/10.3892/ol.2016.4630>
35. Shirakawa K, Kobayashi H, Sobajima J, Hashimoto D, Shimizu A, Wakasugi H. Inflammatory breast cancer: vasculogenic mimicry and its hemodynamics of an inflammatory breast cancer xenograft model. *Breast Cancer Res*. 2003;5(3):136-139. <https://doi.org/10.1186/bcr585>
36. Wilhelm SM, Carter C, Tang L, et al. BAY 43-9006 exhibits broad spectrum oral antitumor activity and targets the RAF/MEK/ERK pathway and receptor tyrosine kinases involved in tumor progression and angiogenesis. *Cancer Res*. 2004;64(19):7099-7109. <https://doi.org/10.1158/0008-5472.CAN-04-1443>
37. Eichholz A, Merchant S, Gaya AM. Anti-angiogenesis therapies: their potential in cancer management. *Onco Targets Ther*. 2010;24(3):69-82. <https://doi.org/10.2147/ott.s5256>
38. Yadav A, Kumar B, Teknos TN, Kumar P. Sorafenib enhances the antitumor effects of chemoradiation treatment by downregulating ERCC-1 and XRCC-1 DNA repair proteins. *Mol Cancer Ther*. 2011;10(7):1241-1251. <https://doi.org/10.1158/1535-7163.MCT-11-0004>

SUPPORTING INFORMATION

Additional supporting information may be found online in the Supporting Information section.

How to cite this article: Almahmoudi R, Salem A, Hadler-Olsen E, Svineng G, Salo T, Al-Samadi A. The effect of interleukin-17F on vasculogenic mimicry in oral tongue squamous cell carcinoma. *Cancer Sci*. 2021;112:2223-2232. <https://doi.org/10.1111/cas.14894>